



## Review Article

# An overview of artificial intelligence in medical physics and radiation oncology



Jiali Liu<sup>1,2,†</sup>, Haonan Xiao<sup>3,†</sup>, Jiawei Fan<sup>4,5,6</sup>, Weigang Hu<sup>4,5,6</sup>, Yong Yang<sup>7</sup>, Peng Dong<sup>7</sup>, Lei Xing<sup>7</sup>, Jing Cai<sup>3,\*</sup>

<sup>1</sup> Department of Clinical Oncology, The University of Hong Kong-Shenzhen Hospital, Shenzhen, China

<sup>2</sup> Department of Clinical Oncology, Hong Kong University Li Ka Shing Medical School, Hong Kong, China

<sup>3</sup> Department of Health Technology and Informatics, The Hong Kong Polytechnic University, Hong Kong, China

<sup>4</sup> Department of Radiation Oncology, Fudan University Shanghai Cancer Center, Shanghai, China

<sup>5</sup> Department of Oncology, Shanghai Medical College, Fudan University, Shanghai, China

<sup>6</sup> Shanghai Key Laboratory of Radiation Oncology, Shanghai, China

<sup>7</sup> Department of Radiation Oncology, Stanford University, CA, USA

## ARTICLE INFO

## Keywords:

Artificial intelligence  
Radiotherapy  
Medical physics

## ABSTRACT

Artificial intelligence (AI) is developing rapidly and has found widespread applications in medicine, especially radiotherapy. This paper provides a brief overview of AI applications in radiotherapy, and highlights the research directions of AI that can potentially make significant impacts and relevant ongoing research works in these directions. Challenging issues related to the clinical applications of AI, such as robustness and interpretability of AI models, are also discussed. The future research directions of AI in the field of medical physics and radiotherapy are highlighted.

## 1. Introduction

In recent years, artificial intelligence (AI) is revolutionizing medical science and healthcare.<sup>1,2</sup> The deep learning applications in radiation oncology and medical physics appeared in the 2016 Annual Meeting of American Association of Physicists in Medicine.<sup>3,4</sup> Since the pioneering applications of deep learning in radiation therapy in 2016 and 2017 by the Stanford group,<sup>3,8</sup> there has been surging interest in the applications of AI in radiation oncology.<sup>9–11</sup> Indeed, in the area of medical physics and radiation oncology, data-driven solutions are quickly evolving and promise to change our practice. The implication of AI to our field is enormous and all indications suggest that AI will transform the ways that many tasks are done in the clinic. The clinical workflow of radiation therapy is shown in Fig. 1. In general, the process includes imaging simulation, contouring, treatment planning, quality assurance (QA), treatment delivery, and follow-up assessment. In each of the steps, there exist multiple difficult decisions to be made and the decision-making process can be either manual or automatic with AI assistance. In this paper, we provide an overview of the applications of AI in radiation oncology and medical physics. We also discuss the potential clinical benefits and challenges of AI-based approaches.

## 2. AI in Medical Physics and Radiation Oncology

## 2.1. AI for target delineation and organ segmentation

Clinically, one of the important tasks is for radiation oncologists to decide on the volume of the tumor target.<sup>12,13</sup> Because the boundary between normal and tumor tissues in the images can be unclear or blurred for various reasons, it is sometimes difficult for radiation oncologists to determine the clinical target volume (CTV) and decide on how much margin to include for treatment planning. Additionally, the delineations of organs at risk (OARs) are also problematic as the process is labor intensive and time consuming.<sup>5,13</sup> Automated segmentation of OARs would greatly improve the efficiency and operator dependency of the process. Some studies involving AI for target delineation and organ segmentation are summarized in Table 1.

Technically, segmentation is the process of clustering an image into several coherent sub-regions according to the extracted features and classifying each sub-region into one of the pre-determined classes. Segmentation techniques are divided into supervised and unsupervised techniques. The former approach incorporates prior knowledge about the image processing task through training samples.<sup>22</sup> The latter relies

\* Corresponding author.

E-mail address: [jing.cai@polyu.edu.hk](mailto:jing.cai@polyu.edu.hk) (J. Cai).

† These authors contributed equally to this work.

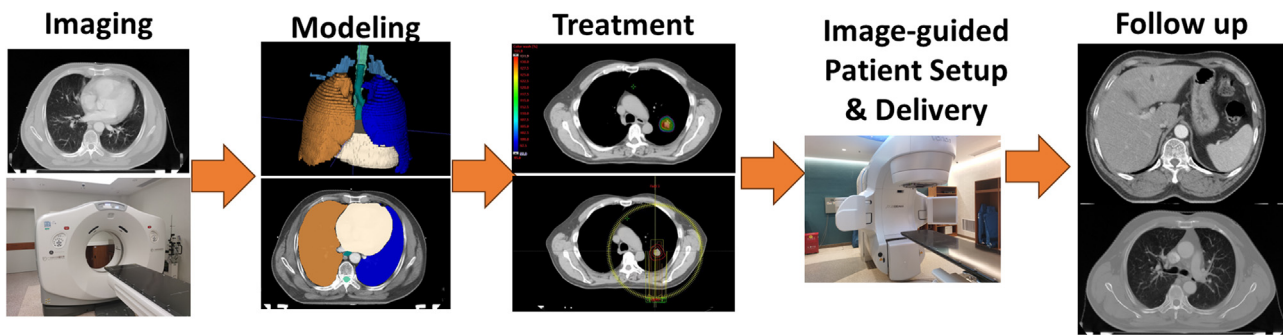


**Fig. 1.** Clinical workflow of radiation therapy. The image provides a comprehensive overview of the process, starting with the acquisition of medical images which are then utilized for modeling. Following this, a treatment plan tailored to the patient's needs is developed. This plan is then implemented, delivering radiation to the patient with the aid of image-guided setup. The final stage involves providing the patient with follow-up care.

**Table 1**

Studies involving artificial intelligence for target delineation and organ segmentation.

| Reference                  | Year | Site           | Architecture | Supervision | Dataset                        | Performance measure |
|----------------------------|------|----------------|--------------|-------------|--------------------------------|---------------------|
| Men et al. <sup>14</sup>   | 2017 | Rectal         | 2D CNN       | Supervised  | CT of 278 patients             | DSC                 |
| Men et al. <sup>15</sup>   | 2017 | Nasopharyngeal | 2D CNN       | Supervised  | CT of 230 patients             | DSC                 |
| Ermis et al. <sup>16</sup> | 2020 | Brain          | 2D DenseNet  | Supervised  | T1w and T2w MRI of 30 patients | DSC                 |
| Jin et al. <sup>17</sup>   | 2020 | Esophageal     | 3D CNN       | Supervised  | CT and PET of 148 patients     | DSC, ASD            |
| Guo et al. <sup>18</sup>   | 2019 | Head and neck  | 3D DenseNet  | Supervised  | CT and PET of 250 patients     | DSC, HD, MSD        |
| Ma et al. <sup>19</sup>    | 2022 | Thoracic       | 3D U-Net     | Supervised  | 4D-CT of 70 patients           | DSC, HD             |
| Momin et al. <sup>20</sup> | 2021 | Thoracic       | 3D R-CNN     | Supervised  | 4D-CT of 49 patients           | DSC, HD95, MSD, VD  |
| Zhou et al. <sup>21</sup>  | 2022 | Abdominal      | 2D ResNet    | Supervised  | 2500 kV X-ray images           | DSC, 3D error       |

Abbreviations: 2D, two dimensional; 3D, three dimensional; ASD, average surface distance; CNN, convolutional neural network; DSC, Dice similarity coefficients; HD, Hausdorff distance; MRI, magnetic resonance imaging; MSD, mean squared difference; PET, positron emission tomography; T1w, T1-weighted; T2w, T2-weighted; VD, volume difference.

on the intensity or gradient analysis of the image via various strategies such as thresholding, graph cut, edge detection, and deformation, to delineate the boundaries of the target object in the image. With the advances in deep learning techniques, significant progress has been made in image segmentation. Noteworthy, deep convolutional neural networks (CNNs) have achieved the state-of-the-art performance for the semantic segmentation of natural images.<sup>23–25</sup> For example, the pioneer studies of Men et al,<sup>14,15</sup> applied fully connected network (FCN) for computed tomography (CT), CTV and OARs segmentation of rectal cancer and nasopharyngeal cancer. They claimed that the deep learning models could complete the segmentation within one minute, facilitating radiotherapy workflow while improving the contouring consistency. In addition to CT, promising results were also achieved on other imaging modalities, including magnetic resonancing imaging (MRI) of various contrasts<sup>16,26</sup> and positron emission tomography (PET).<sup>17,18</sup> Readers are recommended for the seminal paper of Litjens et al.,<sup>27</sup> which reviewed the major concepts of deep learning and over 300 contributions to medical image analysis including image classification, object detection, segmentation, registration and other tasks per application area: neuro, retinal, pulmonary, digital pathology, breast, cardiac, abdominal, musculoskeletal. In addition, Seo et al.<sup>13</sup> reviewed the applications of machine learning techniques, including deep learning, 7–12 kernel support vector machines (SVMs), Markov random fields (MRFs), random forests (RFs), etc., in medical image segmentation only.

In summary, AI-assisted target delineation and organ segmentation showed great potential in improving clinical efficiency and consistency. However, there are also challenges of such method that require future work of the community. First, the scarcity and inconsistency of annotated data may hinder the development of AI models. Preparing large training dataset is not only labor-intensive, but also vulnerable to inter-physician variability. Building benchmark datasets from multiple clinical centers might be a solution to standardizing the model development and performance. Second, AI models usually predict target definition based on a single image modality, while in the clinic physicians usu-

ally combine the information from several image modalities. Integrating anatomical and functional images in AI models can also be an interesting research topic for the community.

## 2.2. AI for image registration

Image registration is a common tool in the clinic and has been widely applied in various tasks, including motion tracking and modeling,<sup>28</sup> segmentation,<sup>29</sup> image-guided treatment,<sup>30</sup> and adaptive radiation therapy.<sup>31</sup> Despite those promising applications, conventional image registration, especially deformable image registration (DIR), relies on iterative optimization algorithms and can take hours for an accurate registration.<sup>32</sup> AI-assisted image registration takes a single forward calculation in implementation, which greatly accelerates the progress. Some studies involving AI for image registration are summarized in Table 2.

Specifically, AI in image registration can be classified into three major categories: deep iterative registration models, supervised registration models, and unsupervised registration models.<sup>52</sup> For deep iterative registration models, CNNs are utilized to replace conventional intensity-based cost function, which is robust to image artifacts and capable of capturing underlying image features. For example, Simonovsky et al.<sup>33</sup> trained a CNN model to distinguish whether two images were well-aligned, and then replaced the intensity-based cost function in brain MRI registration with the CNN model, resulting in significantly improved accuracy. For supervised registration models, they follow the straightforward idea of AI, which utilizes annotated data for training. However, as ground truth deformation is usually not available, the supervision of AI models can also sometimes be artificial, indirect, or a mixture of multiple components. For example, Teng et al.<sup>37</sup> developed a patch-based CNN model for lung 4D-CT and 4D-cone-beam computed tomography (4D-CBCT) registration, whose reference deformations were from VelocityAI (Varian). To overcome the shortage and inaccuracy of reference deformations, Sokooti et al.<sup>38,40</sup> trained AI models with artificially generated deformations and achieved comparable accu-

**Table 2**  
Studies involving artificial intelligence for image registration.

| Reference                         | Year | Site     | Architecture | Supervision     | Dataset  | Performance measure |
|-----------------------------------|------|----------|--------------|-----------------|--|---------------------|
| Simonovsky et al. <sup>33</sup>   | 2016 | Brain    | 3D CNN       | Deep metrics    | IXI, <sup>34</sup> ALBERTs <sup>35</sup>   | DSC                 |
| Sedghi et al. <sup>36</sup>       | 2020 | Brain    | 3D DenseNet  | Deep metrics    | IXI <sup>34</sup>  | FRE, DSC            |
| Teng et al. <sup>37</sup>         | 2021 | Thoracic | 3D CNN       | Supervised      | 4D-CBCT and 4D-CT of 6 patients  | RMSE, SSIM, CC      |
| Sokooti et al. <sup>38</sup>      | 2017 | Thoracic | 3D CNN       | Supervised      | SPREAD <sup>39</sup>   | TRE, Jaco. Det.     |
| Sokooti et al. <sup>40</sup>      | 2019 | Thoracic | 3D CNN       | Supervised      | SPREAD <sup>39</sup>   | TRE, Jaco. Det.     |
| Li et al. <sup>41</sup>           | 2019 | Brain    | 3D CNN       | Semi-supervised | Brain MRI of 3 249 patients  | MI, DSC             |
| Fan et al. <sup>42</sup>          | 2019 | Brain    | 3D CNN       | Supervised      | LONI LPBA40 <sup>43</sup>  | DSC                 |
| Balakrishnan et al. <sup>32</sup> | 2019 | Brain    | 3D U-Net     | Unsupervised    | OASIS, <sup>44</sup> ABIDE, <sup>45</sup> ADHD200, <sup>46</sup> MCIC, <sup>47</sup> PPMI, <sup>48</sup> HABS, <sup>49</sup> Harvard GSP, <sup>50</sup> FreeSurfer Buckner40 <sup>51</sup> | DSC                 |

Abbreviations: 2D, two dimensional; 3D, three dimensional; 4D, four dimensional, CBCT, cone-beam computed tomography; CC, cross-correlation coefficient; CNN, convolutional neural network; CT, computed tomography; DSC, Dice similarity coefficients; FRE, fiducial registration error; Jaco. Det., Jacobian determinant; MI, mutual information; MRI, magnetic resonance imaging; RMSE, root mean squared error; SSIM, structure similarity index measure; TRE, target registration error.

racy with conventional methods across multiple datasets. As for indirect supervisions, Li et al.<sup>41</sup> developed hybrid CNNs that predicts image segmentation and registration together, while the segmentation can in turn aid the registration process. In addition, Fan et al.<sup>42</sup> utilized a mixture of reference deformation and image similarity as supervision, achieving up to a 4% higher average Dice score and more than 30 times faster implementation speed compared with conventional methods like SyN. Unsupervised registration models omitted the time-consuming data preparation process and showed a more convenient way for registration model training. For example, Balakrishnan et al.<sup>32</sup> trained a U-Net-like model for brain MRI registration using intensity-based loss functions, including mean square error and normalized cross-correlation, and achieved comparable Dice score with conventional methods like Syn and NiftyReg, but with more than 20,000 times faster implementation with graphics processing unit (GPU) acceleration. However, without the guidance of reference deformations, the regularization of the deep learning model could be challenging and folding voxels might be more than those in conventional methods if inappropriate loss functions were chosen.

In summary, AI-assisted models can greatly accelerate the implementation of image registration while keeping comparable or even better accuracy. However, there also remains several challenges that need to be addressed. First, shortage of high-quality training data is always a challenge for AI models, and this is even more severe for registration models since ground truth deformation is usually not available. Second, the plausibility of the deformation is another challenge. Deformation regularization is usually just smoothness, which may not be enough for sliding motions. Some conventional methods have tried to solve this,<sup>53</sup> but few AI-assisted models touched this topic. Further research on these is needed to facilitate the AI-assisted registration model development and implementation.

### 2.3. Deep learning-based image reconstruction

Deep learning is used to extract the features difficult to find by human beings and achieve state-of-the-art performance in many imaging tasks. Reconstruction of images (CT, MRI, PET, and so forth) can be improved by deep learning. For example, Zhu et al. developed a deep learning model named AUTOMAP for image reconstruction from k-space.<sup>54</sup> Their findings indicate that their model outperformed conventional reconstruction methods, including compressed sensing, by achieving a more than twice higher signal-to-noise ratio, halving the root mean squared error, and exhibiting fewer artifacts. In current image reconstruction, the sensory or measurement data are converted to an image by model-based method or analytical inversion. For CT imaging, for example, one measures 800 to 1 000 projections from different directions and then performs the reconstruction. With deep learning, we are provided with a wonderful framework to leverage prior patient data for

sparse and artifacts-free CT imaging.<sup>55–58</sup> Some studies involving AI for image reconstruction were summarized in Table 3.

In deep learning-based sparse image reconstruction, the demand for measurement data can be reduced substantially without compromising the quality of resultant images. Different from the conventional image reconstruction method, in which every patient is a new patient with the image reconstruction starting from the very beginning without consideration of prior imaging data, the information extracted from prior data to facilitate the imaging of a new patient is considered. In this way, high-quality imaging with fewer measurements become possible. Recently, Shen, Zhao and Xing<sup>58</sup> have developed a novel deep neural network for ultra-sparse CT image reconstruction. They demonstrated the feasibility of CT imaging by using a single projection. They firstly proposed a deep learning model to generate volumetric tomographic X-ray images from a single projection view for upper-abdomen, lung and head-and-neck, as shown in Fig. 2.<sup>58</sup> Then they proposed a geometry-informed deep learning framework integrating geometric priors of the imaging system which is essential to enhance the performance.<sup>58</sup> A team at Stanford Radiology developed an artificial intelligence-enabled PET imaging technique to synthesize standard-dose amyloid PET images of high quality from ultra-low dose PET images. The synthesized images have similar accuracy (around 90%) for amyloid status to intrareader reproducibility of full-dose images,<sup>61,62</sup> which may represent a significant step forward in PET imaging with multiple-fold reduction of the radionuclide tracers.

In summary, deep learning models have achieved great successes in image reconstruction, especially in the efficiency. However, reconstruction models also face similar challenges as other models. First, models trained on data from a single or a few medical centers may not be generalizable to other centers, and re-training for each center can be time- and resource-consuming. Recently, federated learning has been introduced to medical imaging,<sup>63</sup> which is promising for model development in small medical centers. Second, the reliability of reconstruction models needs thorough evaluation. Although image details can be reconstructed by AI models, unrealistic or extra structures sometimes are also generated. Turing test might be a good way to evaluation the models before applications.<sup>64,65</sup>

### 2.4. AI for dose prediction and automated treatment planning

While numerous clinical studies have clearly shown the significant benefit of tumor dose escalation and hypofractionation, how to efficiently deliver a tumoricidal radiation dose to the tumor without increasing the radiation toxicity remains to be the single most significant challenge in radiation oncology. Treatment planning is an important step in radiation therapy and critically determines the quality of treatment. Currently, the clinical treatment planning process is rather tedious and labor-intensive, yet has no guarantee of generating truly optimal treatment plans. The deficiencies in treatment planning are caused by

**Table 3**  
Studies involving artificial intelligence for image reconstruction.

| Reference                    | Year | Site                | Architecture | Supervision | Dataset  | Performance measure   |
|------------------------------|------|---------------------|--------------|-------------|--|-----------------------|
| Zhu et al. <sup>54</sup>     | 2018 | Brain               | 2D CNN       | Supervised  | ImageNet, <sup>59</sup> MGH-USC HCP <sup>60</sup>  | SNR, RMSE             |
| Shen et al. <sup>58</sup>    | 2019 | Abdominal, thoracic | 3D CNN       | Supervised  | CT of 3 patients                                   | MAE, RMSE, SSIM, PSNR |
| Wu et al. <sup>57</sup>      | 2019 | Knee                | 3D CNN       | Supervised  | MRI of 360 patients                                | SSIM                  |
| Mardani et al. <sup>56</sup> | 2018 | Pediatric, knee     | 3D GAN       | Supervised  | MRI of 350 pediatric patients and 19 knee patients | SNR, SSIM             |
| Chen et al. <sup>61</sup>    | 2018 | Brain               | 2D U-Net     | Supervised  | PET and MRI of 39 patients                         | PSNR, SSIM, RMSE      |
| Ouyang et al. <sup>62</sup>  | 2019 | Brain               | 2D GAN       | Supervised  | PET of 39 patients                                 | PSNR, SSIM, RMSE      |

Abbreviations: 2D, two dimensional; 3D, three dimensional; CNN, convolutional neural network; CT, computed tomography; GAN, generative adversarial network; MAE, mean absolute error; MRI, magnetic resonance imaging; PET, positron emission tomography; PSNR, peak signal-to-noise ratio; RMSE, root mean squared error; SNR, signal-to-noise ratio; SSIM, structure similarity index measure.

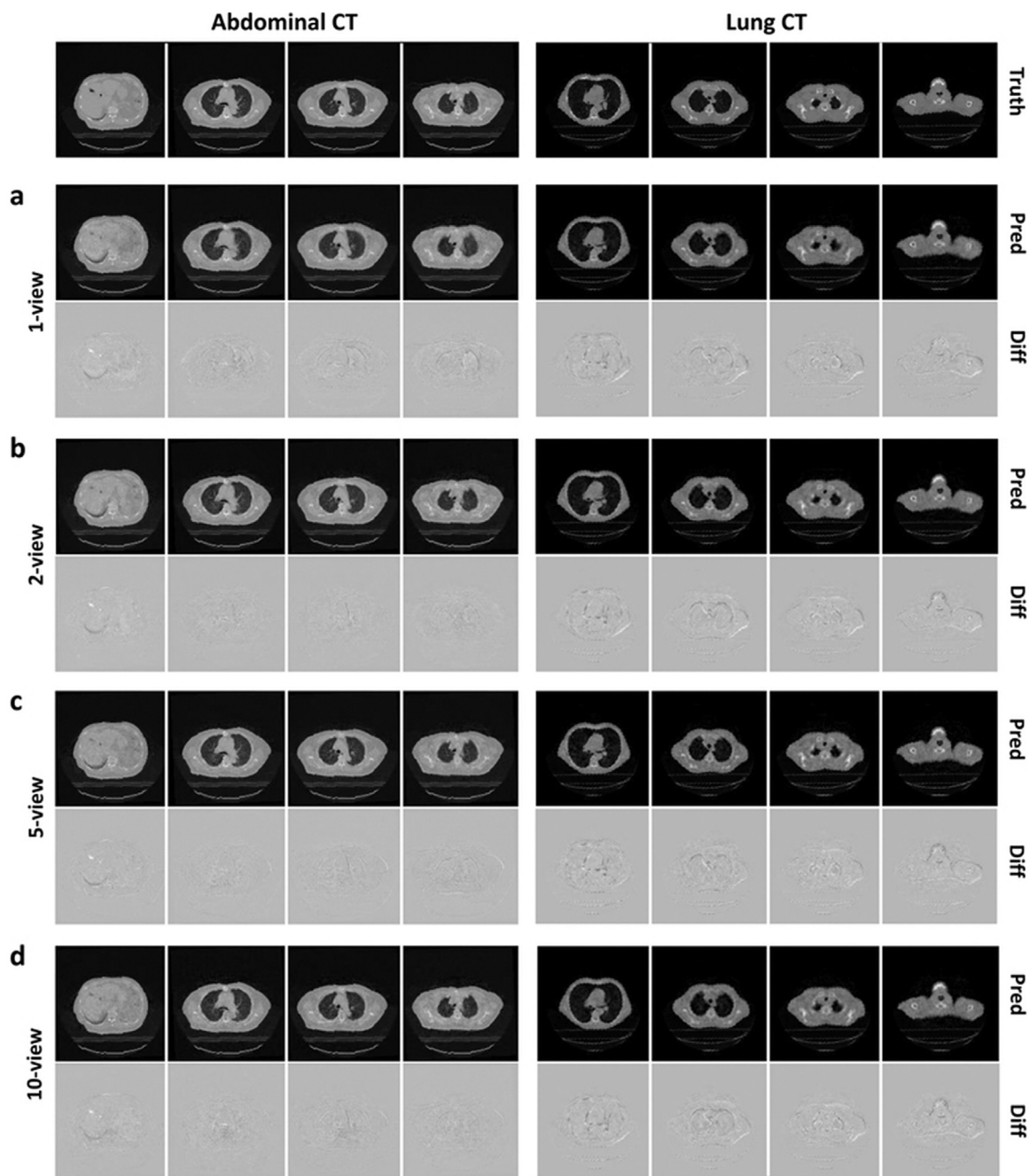


**Fig. 2.** Illustrative instances extracted from the abdominal-CT and lung-CT cases. The prediction using different numbers of 2D projections. Reconstructing images using 1, 2, 5, 10 projection views. In the abdominal-CT case, a total of 720 images were utilized for training, 180 for validation, and 600 for testing. Similarly, for the lung-CT case, 2400 images were used for training, 600 for validation, and 200 for testing. CT, computed tomography.



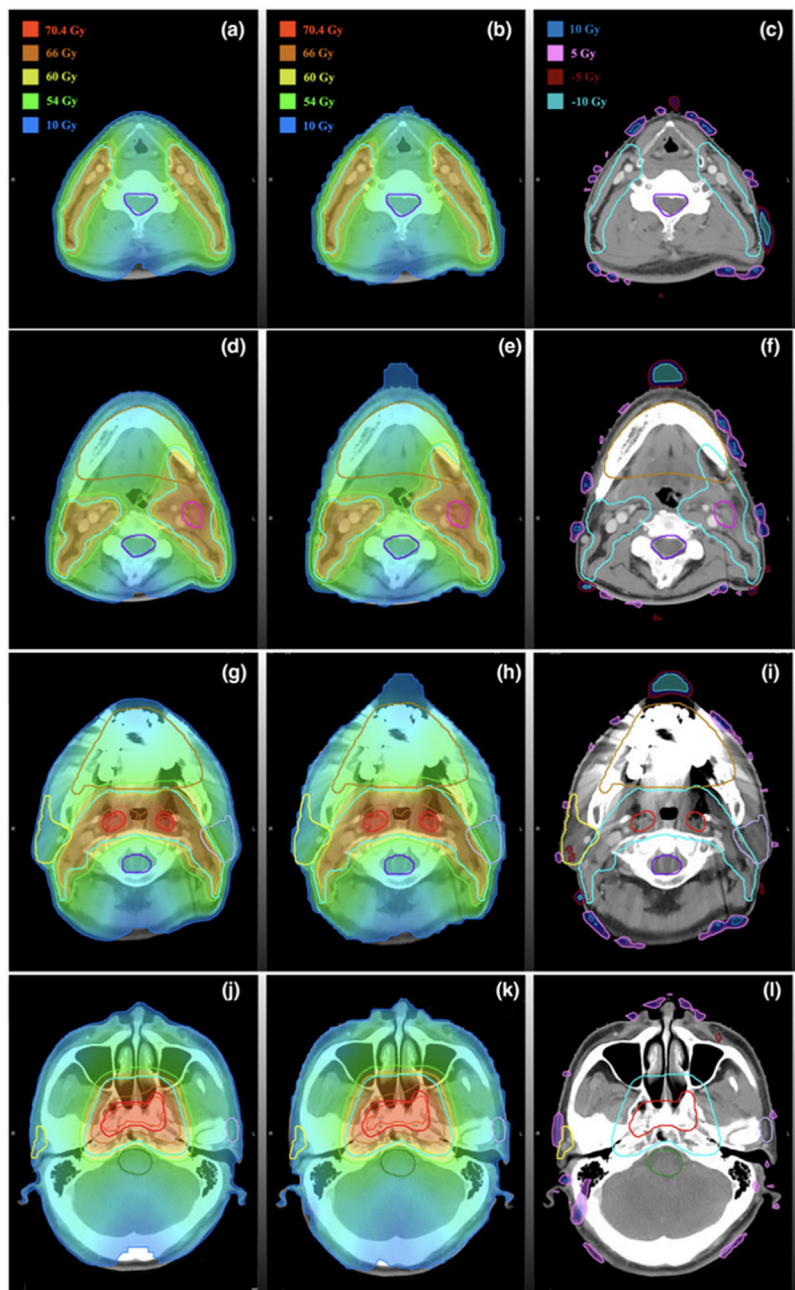


**Fig. 3.** The dose distribution and DVHs comparison between the predicted plan and the automatically generated plan for patient. The upper left (a, d, g, j) is the predicted plan, the upper middle is the automatically generated plan (b, e, h, k), and the upper right is the voxel-by-voxel difference maps (c, f, i, l). The color bars representing different dose levels are shown at the top of the figure. The bottom two plots (m, n) offer a comparative view of the DVHs for both plans, with color bars representing DVHs of different structures. The solid line represents the predicted plan, and the dashed line signifies the automatically generated plan. Used with permission of John Wiley and Sons, copyright 2018; permission conveyed through Copyright Clearance Center, Inc.<sup>68</sup> DVHs, dose-volume histograms.

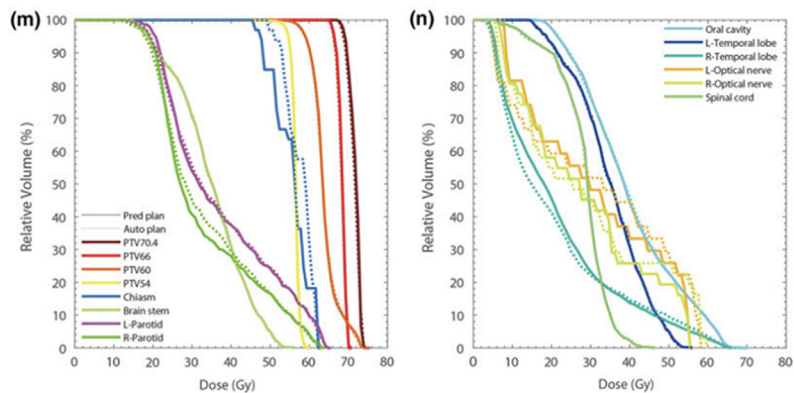


**Table 4**  
Studies involving artificial intelligence for dose prediction and automated treatment planning.

| Reference                   | Year | Site                                 | Architecture | Supervision | Dataset                    | Performance measure              |
|-----------------------------|------|--------------------------------------|--------------|-------------|----------------------------|----------------------------------|
| Mardani et al. <sup>3</sup> | 2016 | Prostate                             | Auto-encoder | Supervised  | 125 prostate patients      | Iso-dose surface overlap         |
| Ma et al. <sup>66</sup>     | 2019 | Prostate                             | 3D CNN       | Supervised  | 70 prostate patients       | SAR                              |
| Ma et al. <sup>67</sup>     | 2019 | Prostate                             | 3D CNN       | Supervised  | 70 prostate patients       | SAR                              |
| Fan et al. <sup>68</sup>    | 2018 | Head and Neck                        | 3D CNN       | Supervised  | 270 head and neck patients | DVH                              |
| Dong et al. <sup>69</sup>   | 2019 | Lung, Brain, Abdomen, Pelvis         | 2D CNN       | Supervised  | 10 patients                | MSE, Gamma index                 |
| Fan et al. <sup>70</sup>    | 2020 | Nasopharyngeal, Lung, Rectum, Breast | 3D U-Net     | Supervised  | 247 patients               | Per-voxel bias, Clinical indices |

Abbreviations: 2D, two dimensional; 3D, three dimensional; CNN, convolutional neural network; DVH, dose-volume histogram; MSE, mean squared error; SAR, sum of absolute residuals.

the involvement of multiple model parameters, which must be determined via manual trial-and-error as their influence on the final dose distribution is patient-dependent and not known until optimization is done. Thus, treatment planning remains to be one of the most labor-intensive and time-consuming tasks in current RT practice, with the quality of the final plan depending heavily on the planner’s training and skills. A more reliable, faster and more autonomous planning approach is urgently needed to greatly improve the safety, quality, efficiency, and cost-effectiveness of radiation therapy. Some studies involving AI for dose prediction and automated treatment planning were summarized in Table 4.

AI-augmented autonomous treatment planning promises to mitigate the bottleneck to maximize the therapeutic ratio of modern radiation therapy. Since the initial work on deep learning-based intensity-modulated radiation therapy (IMRT) dose prediction by Mardani et al.,<sup>3</sup> many attempts have been made to automate treatment planning (Fig. 3).<sup>66-68,71,72</sup> Technically, there are a number of important problems that must be resolved before the deep learning-based techniques can be employed to facilitate clinical treatment. These include, for example, 1) development and clinical implementation of AI-based dose prediction with the incorporation of prior clinical knowledge. Zhao et al. proposed a dose distribution prediction model integrating anatomic features and dosimetric features based on deep learning method, as shown in Fig. 3<sup>66,67</sup>; 2) development of computer algorithm to mimic operations of a human planner to automatically update treatment plan parameters. One of the algorithm frameworks is shown in Fig. 4;<sup>71</sup> 3) implementation of deep learning-based dose calculation to speed up the planning process, as shown in Fig. 5.<sup>69,70</sup> AI-augmented treatment planning will not only speed up the treatment planning process, but also improve the quality of treatment plans, and help to standardize the treatment planning procedure.

Several specific challenges still remain for AI-augmented treatment planning. First, the models usually treat the dose prediction to each anatomical structures as separate tasks and neglect the relationship between maximizing target dose and minimizing OAR doses.<sup>73,74</sup> Second, some studies focused on dose map prediction only, yet did not cover the delivery parameters, including beam angles and fluencies. Research to address these tasks are therefore encouraged.

### 2.5. Deep learning-augmented image guidance

Another important example of AI is to provide better image guidance tools for radiation therapy, where nearly real-time information about the tumor target as well as patient setup is necessary to achieve accurate beam targeting. Recent advances in radiotherapy techniques, including volumetric modulated arc therapy (VMAT), IMRT, stereotactic radiosurgery (SRS), and stereotactic ablative radiotherapy (SABR), provide effective ways to generate steep dose distributions at the target boundary while sparing the healthy issues. However, these steep dose distributions call for stringent requirements for enhanced target positioning.

Radiation treatment machine systems with image guidance have been routinely used in clinical practice.<sup>75-82</sup> Deep learning enables

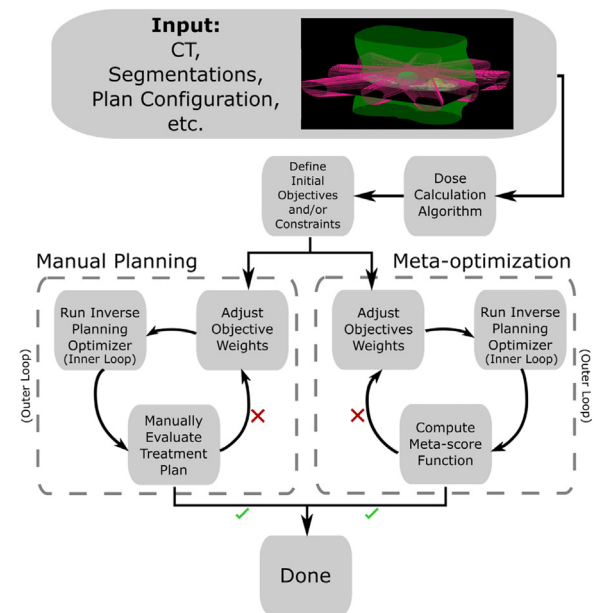


**Fig. 4.** Visualization of meta-optimized workflow compared to manual treatment planning. Both the manual treatment planning and the meta-optimized workflow are structured as two nested loops of optimization. The inner loop involves inverse planning optimization, which includes processes such as fluence map optimization and direct aperture optimization. The outer loop, on the other hand, is where either meta-optimization or manual optimization of hyperparameters takes place. Used with permission of IOP Publishing Ltd, copyright 2022; permission conveyed through Copyright Clearance Center, Inc.<sup>71</sup> CT, computed tomography.

learning semantic features and understanding complex relationships from data.<sup>83</sup> This has greatly augmented the applications of AI in image-guided radiation therapy (IGRT). Zhao et al. employed deep learning to localize the prostate target on kV X-ray images, as shown in Fig. 6.<sup>10</sup> Differences between the predicted target positions and their actual positions are  $1.58 \pm 0.43$  mm,  $1.64 \pm 0.43$  mm, and  $1.67 \pm 0.36$  mm in anterior-posterior, lateral, and oblique directions for prostate tumor.<sup>10,84,85</sup> which demonstrated highly accurate, markerless prostate localization based on deep learning are achievable. AI also provides better solutions to motion management<sup>86-88</sup> and quality assurance<sup>89-97</sup> in radiation therapy.

Real-time target tracking requires a latency from motion to treatment response of less than 500 ms,<sup>98</sup> and abovementioned studies all satisfied this criterion. However, there are more potential latencies that have to be considered. For example, although only a single slice was needed in some studies, image reconstruction of that slice can still take a while. Besides, the transfer of raw data from the image scanner to the workstation for processing is also a non-negligible component. Prospective studies including the entire treatment process is therefore encouraged for evaluation.

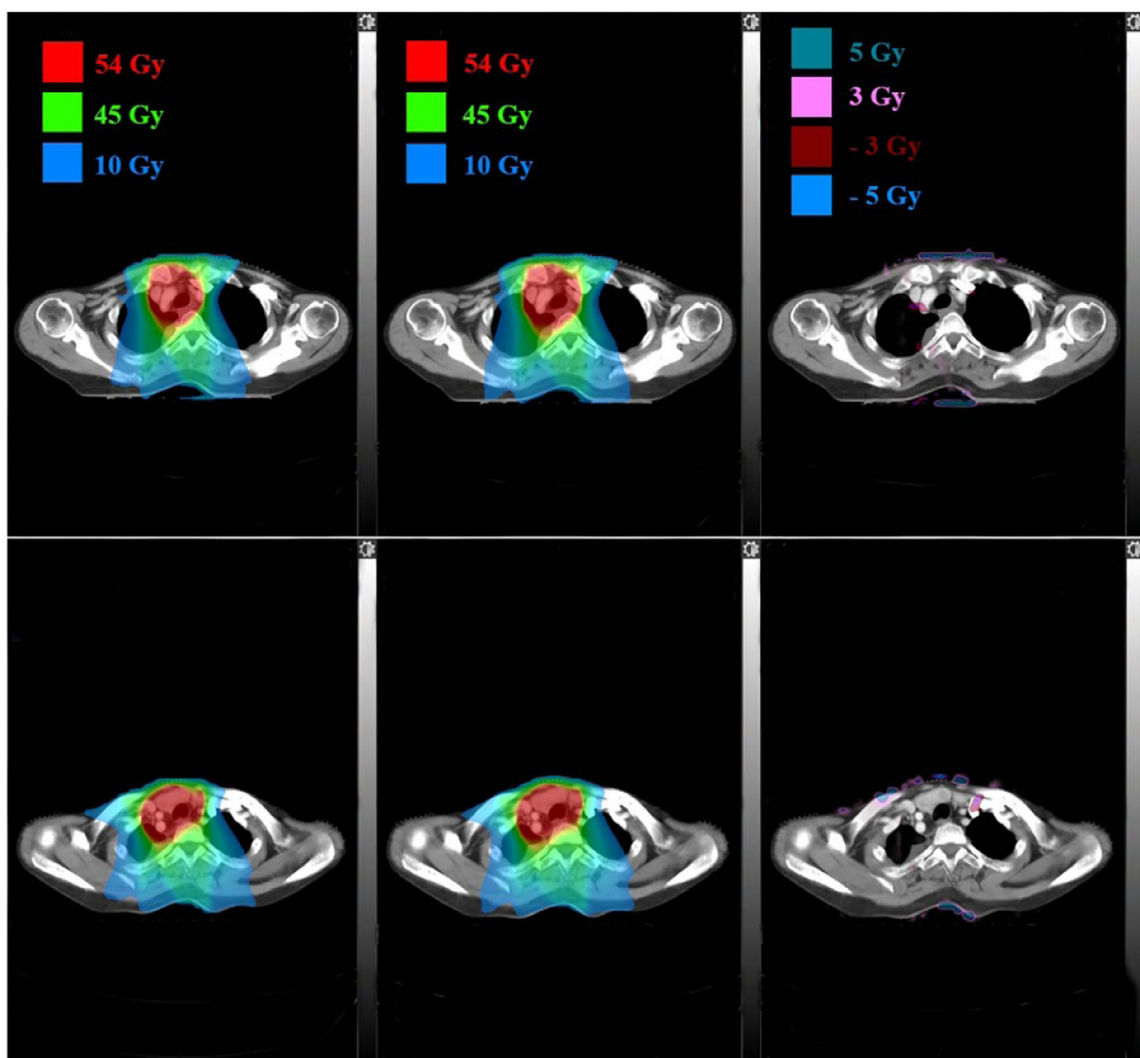


**Fig. 5.** Dose distributions comparison in two axial planes for a lung patient. The figure displays the dose distributions as calculated by both the treatment planning system and deep learning, along with the pixel-wise differences between these two calculations. The left side of the figure represents the dose distribution as calculated by the treatment planning system, the middle section depicts the dose distribution as calculated by deep learning, and the right side illustrates the pixel-wise differences between the two calculations. Used with permission of IOP Publishing, Ltd, copyright 2020; permission conveyed through Copyright Clearance Center, Inc.<sup>70</sup>

**Table 5**  
Studies involving artificial intelligence for outcome prediction.

| Reference                           | Year | Site       | Architecture      | Supervision | Dataset                          | Performance measure  |
|-------------------------------------|------|------------|-------------------|-------------|----------------------------------|----------------------|
| Ibragimov et al. <sup>99</sup>      | 2018 | Liver      | 3D CNN            | Supervised  | 125 liver SBRT cases             | ROC curve            |
| Ibragimov et al. <sup>100</sup>     | 2020 | Liver      | 3D CNN            | Supervised  | 122 liver SBRT cases             | Accuracy, risk score |
| Jean-Emmanuel et al. <sup>101</sup> | 2020 | Colorectal | Gradient-boosting | Supervised  | 2 359 colorectal cancer patients | ROC curve, accuracy  |
| Liu et al. <sup>102</sup>           | 2021 | Lung       | LSTM              | Supervised  | 104 lung cancer patients         | ROC curve            |

Abbreviations: 3D, three dimensional; CNN, convolutional neural network; LSTM, long short-term memory; SAR, sum of absolute residuals; SBRT, stereotactic body radiation therapy; ROC curve, receiver operating characteristic curve.

### 2.6. Deep learning-based outcome prediction

Deep learning-based process prediction models gained much popularity and led to breakthrough results in a variety of applications. Some studies involving AI for outcome prediction were summarized in Table 5. Ibragimov et al.<sup>99</sup> predicted the patient survival and local progression after stereotactic body radiation therapy using 3D dose analysis based on deep learning. Moreover, they proposed a deep learning based model to recognize the toxicity risk map for the abdominal areas, as shown in Fig. 7.<sup>100</sup> Jean-Emmanuel et al.<sup>101</sup> provided an explainable prediction of the 10-year death rate of colorectal cancer (CRC) us-

ing XGBoost python package with tumor features, and patients' medical and demographic information. The area under the receiver operating characteristic (AUC) of this model was  $0.84 \pm 0.04$  and the accuracy was  $0.83 \pm 0.04$ . Liu et al.<sup>102</sup> developed an individualized deep-learning based model by using the whole dose information contained in dose-volume histograms (DVHs) instead of some isolated index, like V20, V40, etc., to predict lymphopenia, which takes into account the isodose distribution.

With the increasing availability of high-quality clinical data and state-of-the-art deep learning infrastructure, we anticipate that exciting and clinically useful models will be readily available in the near future.



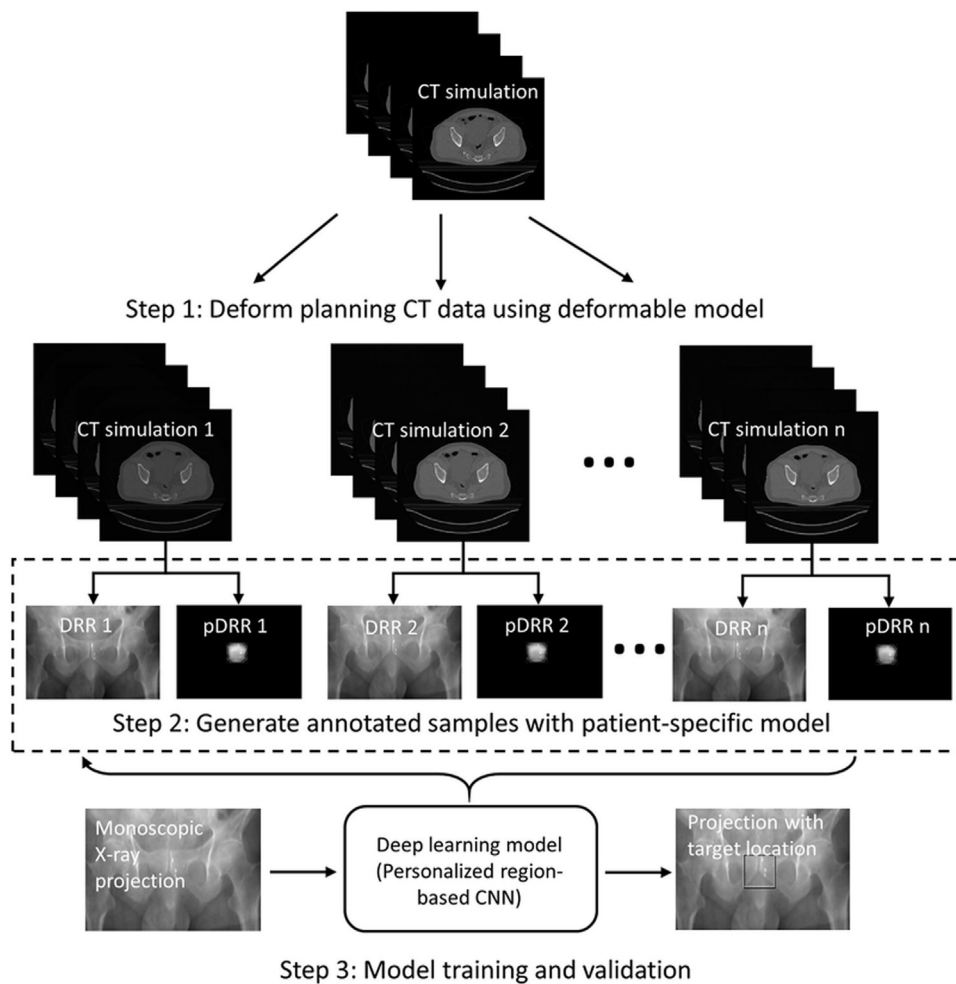


**Fig. 6.** Overall flowchart of the proposed deep learning-based treatment target localization method. The method involves several steps: (1) The patient’s pCT images are placed in OBI geometry. (2) A series of changes, including translations, rotations, and deformations, are introduced to the pCT images to simulate different clinical scenarios. For each of the changes made, a DRR image that includes the corresponding prostate contour and bounding box is generated. These annotations are used to train a deep learning model for the subsequent localization of the prostate target. (3) Validation tests are performed using both DRR images and monoscopic X-ray projection images obtained from a kV OBI system. Used with permission of Elsevier Science & Technology Journals, copyright 2019; permission conveyed through Copyright Clearance Center, Inc.<sup>10</sup> CT, computed tomography; CNN, convolutional neural network; DRR, digitally reconstructed radiograph; kV, kilovoltage; OBI, onboard imager; pCT, planning computed tomography; pDRR, prostate digitally reconstructed radiograph.

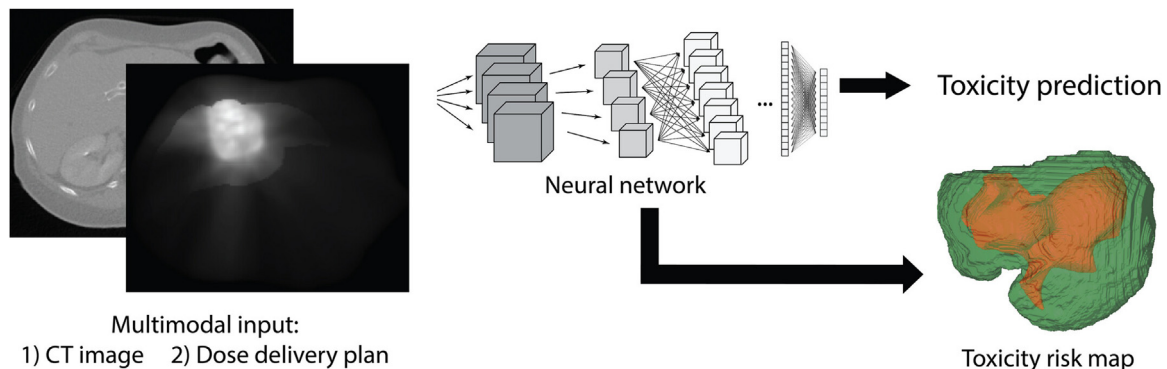


**Fig. 7.** Depiction of the deep learning framework for critical region identification in liver RT. A CNN is trained to discern consistent patterns in pre-RT computed tomography images and the administered RT doses, and to associate these patterns with post-RT toxicity manifestation. The properties of the CNN are then analyzed to identify anatomical regions, the sparing of which significantly correlates with a reduction in toxicity risk. This analysis culminates in the creation of a toxicity risk map for the liver area. Used with permission of John Wiley & Sons - Books, copyright 2020; permission conveyed through Copyright Clearance Center, Inc.<sup>100</sup> CNN, convolutional neural network; RT, radiation therapy.

Despite the promising future, some challenges need to be addressed before the clinical implementation of those models. First, the prediction is usually discrete, like Grade I, II, III, etc. However, treatment response or toxicity are always more complex than the discrete grades.<sup>103</sup> Second, clinical data are inherently multi-modality, including medical images, treatment plans, patients’ physiological parameters, and even patients’ life habits. Current models mostly focus on medical images and treatment plans, which might lose useful information for prediction.

### 2.7. Guidelines for development and clinical trials of AI

Recently, it has become increasingly important to prospectively assess the impact of interventions involving artificial intelligence on health outcomes. The Standard Protocol Items: Recommendations for Interventional Trials-Artificial Intelligence (SPIRIT-AI) extension<sup>104</sup> is a new guideline for reporting clinical trial protocols to evaluate the AI component interventions. The Consolidated Standards of Reporting



Trials-Artificial Intelligence (CONSORT-AI) extension<sup>105</sup> is a new guideline for reporting clinical trials used to evaluate an AI component intervention. A staged consensus process including a literature review and expert consultation was used for the development of both guidelines. Clear descriptions of AI intervention were recommended, including instructions and skills for using, the integrated setting, input and output data handling, the human-AI interaction, and error case analysis. They aimed to increase the transparency and completeness of clinical trials of AI interventions. Luo et al.<sup>106</sup> proposed a set of guidelines for the use of machine learning predictive models in clinical settings, including a reporting item list and practical steps to develop predictive models. They aimed to enable correct application and consistent reporting of machine learning models in clinical settings. Most of the guidelines focus on data privacy and ethics.<sup>107–110</sup> Since we are mainly interested in the development of artificial intelligence tools and the conduct of clinical trials in clinical settings, we will not go into details.

### 3. Conclusions

AI has made remarkable progress in the past decade. It has recently shown expert-level accuracy in various applications and in improving the clinical gain and therapeutic ratio. Deep learning represents one of the most important advances in the history of radiation oncology. The technique holds significant potential to revolutionize radiation oncology research and practice. Despite all the promises, potential pitfalls exist with the current implementation. Noteworthy, AI is still largely a black box with little interpretability, which limits its utility, especially in the area of healthcare. The development of interpretable AI is of paramount importance for the widespread adaptation of AI in healthcare.

### Declaration of competing interest

The authors declare that they have no conflict of interests.

### Consent for publication

The patients whose medical images are presented in this manuscript provided consent for publication of their medical images for the manuscript. Only de-identified data and images are used in this review.

### Acknowledgments

We would like to express our deepest appreciation to Yajun Jia for providing picture material in the process of drafting Fig. 1.

### Author contributions

J.L. and H.X. took on significant roles in the research project, specifically in terms of gathering pertinent papers and drafting the initial manuscript. All authors were actively involved in the process of reviewing and refining the manuscript.

### References

- Xing L, Giger ML, Min JK. *Artificial Intelligence in Medicine*. Academic Press; 2021.
- Huynh E, Hosny A, Guthrie C, et al. Artificial intelligence in radiation oncology. *Nat Rev Clin Oncol*. 2020;17(12):771–781. doi:10.1038/s41571-020-0417-8.
- Mardani M, Dong P, Xing L. Deep-learning based prediction of achievable dose for personalizing inverse treatment planning. *Int J Radiat Oncol Biol Phys*. 2016;96(2):E419–E420. doi:10.1016/j.ijrobp.2016.06.1685.
- Ibragimov B, Pernus F, Strojjan P, et al. TH-CD-206-05: machine-learning based segmentation of organs at risks for head and neck radiotherapy planning. *Med Phys*. 2016;43(6Part46):3883. doi:10.1118/1.4958186.
- Ibragimov B, Xing L. Segmentation of organs-at-risks in head and neck CT images using convolutional neural networks. *Med Phys*. 2017;44(2):547–557. doi:10.1002/mp.12045.
- Ibragimov B, Toesca D, Chang D, et al. Combining deep learning with anatomical analysis for segmentation of the portal vein for liver SBRT planning. *Phys Med Biol*. 2017;62(23):8943–8958. doi:10.1088/1361-6560/aa9262.
- Ibragimov B, Korez R, Likar B, et al. Segmentation of pathological structures by landmark-assisted deformable models. *IEEE Trans Med Imaging*. 2017;36(7):1457–1469. doi:10.1109/TMI.2017.2667578.
- Arik SO, Ibragimov B, Xing L. Fully automated quantitative cephalometry using convolutional neural networks. *J Med Imaging*. 2017;4(1):014501. doi:10.1117/1.JMI.4.1.014501.
- Zhao W, Capaldi D, Chuang C, et al. Fiducial-free image-guided spinal stereotactic radiosurgery enabled via deep learning. *Int J Radiat Oncol Biol Phys*. 2020;108(3):e357. doi:10.1016/j.ijrobp.2020.07.2348.
- Zhao W, Han B, Yang Y, et al. Incorporating imaging information from deep neural network layers into image guided radiation therapy (IGRT). *Radiother Oncol*. 2019;140:167–174. doi:10.1016/j.radonc.2019.06.027.
- Li X, Chen H, Qi X, et al. H-DenseUNet: hybrid densely connected UNet for liver and tumor segmentation from CT volumes. *IEEE Trans Med Imaging*. 2018;37(12):2663–2674. doi:10.1109/TMI.2018.2845918.
- Seo H, Huang C, Bassenne M, et al. Modified U-Net (mU-Net) with incorporation of object-dependent high level features for improved liver and liver-tumor segmentation in CT images. *IEEE Trans Med Imaging*. 2020;39(5):1316–1325. doi:10.1109/TMI.2019.2948320.
- Maes F, Collignon A, Vandermeulen D, et al. Multimodality image registration by maximization of mutual information. *IEEE Trans Med Imaging*. 1997;16(2):187–198. doi:10.1109/42.563664.
- Men K, Dai J, Li Y. Automatic segmentation of the clinical target volume and organs at risk in the planning CT for rectal cancer using deep dilated convolutional neural networks. *Med Phys*. 2017;44(12):6377–6389. doi:10.1002/mp.12602.
- Men K, Chen X, Zhang Y, et al. Deep deconvolutional neural network for target segmentation of nasopharyngeal cancer in planning computed tomography images. *Front Oncol*. 2017;7:315. doi:10.3389/fonc.2017.00315.
- Ermis E, Jungo A, Poel R, et al. Fully automated brain resection cavity delineation for radiation target volume definition in glioblastoma patients using deep learning. *Radiat Oncol*. 2020;15(1):100. doi:10.1186/s13014-020-01553-z.
- Jin D, Guo D, Ho TY, et al. DeepTarget: gross tumor and clinical target volume segmentation in esophageal cancer radiotherapy. *Med Image Anal*. 2021;68:101909. doi:10.1016/j.media.2020.101909.
- Guo Z, Guo N, Gong K, et al. Gross tumor volume segmentation for head and neck cancer radiotherapy using deep dense multi-modality network. *Phys Med Biol*. 2019;64(20):205015. doi:10.1088/1361-6560/ab440d.
- Ma Y, Mao J, Liu X, et al. Deep learning-based internal gross target volume definition in 4D CT images of lung cancer patients. *Med Phys*. 2023;50(4):2303–2316. doi:10.1002/mp.16106.
- Momin S, Lei Y, Tian Z, et al. Lung tumor segmentation in 4D CT images using motion convolutional neural networks. *Med Phys*. 2021;48(11):7141–7153. doi:10.1002/mp.15204.
- Zhou D, Nakamura M, Mukumoto N, et al. Development of a deep learning-based patient-specific target contour prediction model for markerless tumor positioning. *Med Phys*. 2022;49(3):1382–1390. doi:10.1002/mp.15456.
- Mao KZ, Zhao P, Tan PH. Supervised learning-based cell image segmentation for p53 immunohistochemistry. *IEEE Trans Biomed Eng*. 2006;53(6):1153–1163. doi:10.1109/TBME.2006.873538.
- Noh H, Hong S, Han B. Learning deconvolution network for semantic segmentation. *2015 IEEE International Conference on Computer Vision (ICCV)*; 2015:1520–1528. doi:10.1109/ICCV.2015.178.
- He K, Zhang X, Ren S, et al. Deep residual learning for image recognition. *2016 IEEE Conference on Computer Vision and Pattern Recognition (CVPR)*; 2016:770–778. doi:10.1109/CVPR.2016.90.
- Huang G, Liu Z, Van Der Maaten L, et al. Densely connected convolutional networks. *2017 IEEE Conference on Computer Vision and Pattern Recognition (CVPR)*; 2017:2261–2269. doi:10.1109/CVPR.2017.243.
- Peeken JC, Molina-Romero M, Diehl C, et al. Deep learning derived tumor infiltration maps for personalized target definition in glioblastoma radiotherapy. *Radiother Oncol*. 2019;138:166–172. doi:10.1016/j.radonc.2019.06.031.
- Litjens G, Kooi T, Bejnordi BE, et al. A survey on deep learning in medical image analysis. *Med Image Anal*. 2017;42:60–88. doi:10.1016/j.media.2017.07.005.
- Christensen GE, Song JH, Lu W, et al. Tracking lung tissue motion and expansion/compression with inverse consistent image registration and spirometry. *Med Phys*. 2007;34(6):2155–2163. doi:10.1118/1.2731029.
- Reed VK, Woodward WA, Zhang L, et al. Automatic segmentation of whole breast using atlas approach and deformable image registration. *Int J Radiat Oncol Biol Phys*. 2009;73(5):1493–1500. doi:10.1016/j.ijrobp.2008.07.001.
- Schreibmann E, Thorndyke B, Li T, et al. Four-dimensional image registration for image-guided radiotherapy. *Int J Radiat Oncol Biol Phys*. 2008;71(2):578–586. doi:10.1016/j.ijrobp.2008.01.042.
- Olteanu LA, Madani I, De Neve W, et al. Evaluation of deformable image coregistration in adaptive dose painting by numbers for head-and-neck cancer. *Int J Radiat Oncol Biol Phys*. 2012;83(2):696–703. doi:10.1016/j.ijrobp.2011.07.037.
- Balakrishnan G, Zhao A, Sabuncu MR, et al. VoxelMorph: a learning framework for deformable medical image registration. *IEEE Trans Med Imaging*. 2019. doi:10.1109/TMI.2019.2897538.
- Simonovsky M, Gutiérrez-Becker B, Mateus D, et al. A deep metric for multimodal registration. In: Ourselin S, Joskowicz L, Sabuncu M, Unal G, Wells W, eds. *Medical Image Computing and Computer-Assisted Intervention - MICCAI 2016*. Lecture Notes in Computer Science. Vol 9902. Springer;2016:10–18. doi:10.1007/978-3-319-46726-9\_2
- Biomedical Image Analysis Group, Imperial College London. IXI dataset. Accessed August 3, 2023. <http://brain-development.org/ixi-dataset/>.

35. Gousias IS, Edwards AD, Rutherford MA, et al. Magnetic resonance imaging of the newborn brain: manual segmentation of labelled atlases in term-born and preterm infants. *Neuroimage*. 2012;62(3):1499–1509. doi:10.1016/j.neuroimage.2012.05.083.
36. Sedghi A, O'Donnell LJ, Kapur T, et al. Image registration: maximum likelihood, minimum entropy and deep learning. *Med Image Anal*. 2021;69:101939. doi:10.1016/j.media.2020.101939.
37. Teng X, Chen Y, Zhang Y, et al. Respiratory deformation registration in 4D-CT/cone beam CT using deep learning. *Quant Imaging Med Surg*. 2021;11(2):737–748. doi:10.21037/qims-19-1058.
38. Sokooti H, De Vos B, Berendsen F, et al. Nonrigid image registration using multi-scale 3D convolutional neural networks. In: Descoteaux M, Maier-Hein L, Franz A, Jannin P, Collins D, Duchesne S, eds. Springer; 2017:232–239. 10433. doi:10.1007/978-3-319-66182-7\_27.
39. Stolk J, Putter H, Bakker EM, et al. Progression parameters for emphysema: a clinical investigation. *Respir Med*. 2007;101(9):1924–1930. doi:10.1016/j.rmed.2007.04.016.
40. Sokooti H, de Vos B, Berendsen F, et al. 3D convolutional neural networks image registration based on efficient supervised learning from artificial deformations. Posted online August 27, 2019. arXiv:1908.10235v1[cs.LG]. doi:10.48550/arXiv.1908.10235.
41. Li B, Niessen WJ, Klein S, et al. A hybrid deep learning framework for integrated segmentation and registration: evaluation on longitudinal white matter tract changes. In: Shen, D, Liu T, Peters TM, et al, eds. Medical Image Computing and Computer Assisted Intervention – MICCAI 2019. MICCAI 2019. Lecture Notes in Computer Science, vol 11766. Springer; 2019:645–653. doi:10.1007/978-3-030-32248-9\_72.
42. Fan J, Cao X, Yap PT, et al. BIRNet: brain image registration using dual-supervised fully convolutional networks. *Med Image Anal*. 2019;54:193–206. doi:10.1016/j.media.2019.03.006.
43. Klein A, Andersson J, Ardekani BA, et al. Evaluation of 14 nonlinear deformation algorithms applied to human brain MRI registration. *Neuroimage*. 2009;46(3):786–802. doi:10.1016/j.neuroimage.2008.12.037.
44. Marcus DS, Wang TH, Parker J, et al. Open Access Series of Imaging Studies (OASIS): cross-sectional MRI data in young, middle aged, nondemented, and demented older adults. *J Cogn Neurosci*. 2007;19(9):1498–1507. doi:10.1162/jocn.2007.19.9.1498.
45. Di Martino A, Yan CG, Li Q, et al. The autism brain imaging data exchange: towards a large-scale evaluation of the intrinsic brain architecture in autism. *Mol Psychiatry*. 2014;19(6):659–667. doi:10.1038/mp.2013.78.
46. Consortium HD. The ADHD-200 consortium: a model to advance the translational potential of neuroimaging in clinical neuroscience. *Front Syst Neurosci*. 2012;6(62):62. doi:10.3389/fnsys.2012.00062.
47. Gollub RL, Shoemaker JM, King MD, et al. The MCIC collection: a shared repository of multi-modal, multi-site brain image data from a clinical investigation of schizophrenia. *Neuroinformatics*. 2013;11(3):367–388. doi:10.1007/s12021-013-9184-3.
48. Marek K, Jennings D, Lasch S, et al. The Parkinson Progression Marker Initiative (PPMI). *Prog Neurobiol*. 2011;95(4):629–635. doi:10.1016/j.pneurobio.2011.09.005.
49. Dagley A, LaPoint M, Huijbers W, et al. Harvard aging brain study: dataset and accessibility. *Neuroimage*. 2017;144(Pt B):255–258. doi:10.1016/j.neuroimage.2015.03.069.
50. Holmes AJ, Hollinshead MO, O'Keefe TM, et al. Brain Genomics Superstruct Project initial data release with structural, functional, and behavioral measures. *Sci Data*. 2015;2(1):150031. doi:10.1038/sdata.2015.31.
51. Fischl B. FreeSurfer. *Neuroimage*. 2012;62(2):774–781. doi:10.1016/j.neuroimage.2012.01.021.
52. Xiao H, Teng X, Liu C, et al. A review of deep learning-based three-dimensional medical image registration methods. *Quant Imaging Med Surg*. 2021;11(12):4895–4916. doi:10.21037/qims-21-175.
53. Vishnevskiy V, Gass T, Szezeky G, et al. Isotropic total variation regularization of displacements in parametric image registration. *IEEE Trans Med Imaging*. 2017;36(2):385–395. doi:10.1109/TMI.2016.2610583.
54. Zhu B, Liu JZ, Cauley SF, et al. Image reconstruction by domain-transform manifold learning. *Nature*. 2018;555(7697):487–492. doi:10.1038/nature25988.
55. Shen L, Zhao W, Capaldi D, et al. A geometry-informed deep learning framework for ultra-sparse 3D tomographic image reconstruction. *Comput Biol Med*. 2022:105710. doi:10.1016/j.combiomed.2022.105710.
56. Mardani M, Gong E, Cheng JY, et al. Deep generative adversarial neural networks for compressive sensing MRI. *IEEE Trans Med Imaging*. 2019;38(1):167–179. doi:10.1109/TMI.2018.2858752.
57. Wu Y, Ma Y, Capaldi DP, et al. Incorporating prior knowledge via volumetric deep residual network to optimize the reconstruction of sparsely sampled MRI. *Magn Reson Imaging*. 2020;66:93–103. doi:10.1016/j.mri.2019.03.012.
58. Shen L, Zhao W, Xing L. Patient-specific reconstruction of volumetric computed tomography images from a single projection view via deep learning. *Nat Biomed Eng*. 2019;3(11):880–888. doi:10.1038/s41551-019-0466-4.
59. Krizhevsky A, Sutskever I, Hinton GE. ImageNet classification with deep convolutional neural networks. *Commun ACM*. 2017;60(6):84–90. doi:10.1145/3065386.
60. Fan Q, Witzel T, Nummenmaa A, et al. MGH-USC human connectome project datasets with ultra-high b-value diffusion MRI. *Neuroimage*. 2016;124(Pt B):1108–1114. doi:10.1016/j.neuroimage.2015.08.075.
61. Chen KT, Gong E, de Carvalho Macruz FB, et al. Ultra-low-dose 18F-florbetaben amyloid PET imaging using deep learning with multi-contrast MRI inputs. *Radiology*. 2019;290(3):649–656. doi:10.1148/radiol.2018180940.
62. Ouyang J, Chen KT, Gong E, et al. Ultra-low-dose PET reconstruction using generative adversarial network with feature matching and task-specific perceptual loss. *Med Phys*. 2019;46(8):3555–3564. doi:10.1002/mp.13626.
63. Nguyen DC, Pham Q-V, Pathirana PN, et al. Federated learning for smart healthcare: a survey. *ACM Computing Surveys*. 2022;55(3):1–37. doi:10.1145/3501296.
64. Li W, Kazemifar S, Bai T, et al. Synthesizing CT images from MR images with deep learning: model generalization for different datasets through transfer learning. *Biomed Phys Eng Express*. 2021;7(2):025020. doi:10.1088/2057-1976/abe3a7.
65. Li W, Xiao H, Li T, et al. Virtual contrast-enhanced magnetic resonance images synthesis for patients with nasopharyngeal carcinoma using multimodality-guided synergistic neural network. *Int J Radiat Oncol Biol Phys*. 2022;112(4):1033–1044. doi:10.1016/j.ijrobp.2021.11.007.
66. Ma M, Kovalchuk N, Buyounouski MK, et al. Incorporating dosimetric features into the prediction of 3D VMAT dose distributions using deep convolutional neural network. *Phys Med Biol*. 2019;64(12):125017. doi:10.1088/1361-6560/ab2146.
67. Ma M, KB M, Vasudevan V, et al. Dose distribution prediction in isodose feature-preserving voxelization domain using deep convolutional neural network. *Med Phys*. 2019;46(7):2978–2987. doi:10.1002/mp.13618.
68. Fan J, Wang J, Chen Z, et al. Automatic treatment planning based on three-dimensional dose distribution predicted from deep learning technique. *Med Phys*. 2019;46(1):370–381. doi:10.1002/mp.13271.
69. Dong P, Xing L. Deep DoseNet: a deep neural network for accurate dosimetric transformation between different spatial resolutions and/or different dose calculation algorithms for precision radiation therapy. *Phys Med Biol*. 2020;65(3):035010. doi:10.1088/1361-6560/ab652d.
70. Fan J, Xing L, Dong P, et al. Data-driven dose calculation algorithm based on deep U-Net. *Phys Med Biol*. 2020;65(24):245035. doi:10.1088/1361-6560/abca05.
71. Huang C, Nomura Y, Yang Y, et al. Meta-optimization for fully automated radiation therapy treatment planning. *Phys Med Biol*. 2022;67(5). doi:10.1088/1361-6560/ac5672.
72. Huang C, Yang Y, Xing L. Fully automated noncoplanar radiation therapy treatment planning. *Med Phys*. 2021;48(11):7439–7449. doi:10.1002/mp.15223.
73. Li H, Peng X, Zeng J, et al. Explainable attention guided adversarial deep network for 3D radiotherapy dose distribution prediction. *Knowl-Based Syst*. 2022;241:108324. doi:10.1016/j.knsys.2022.108324.
74. Yue M, Xue X, Wang Z, et al. Dose prediction via distance-guided deep learning: Initial development for nasopharyngeal carcinoma radiotherapy. *Radiother Oncol*. 2022;170:198–204. doi:10.1016/j.radonc.2022.03.012.
75. Zhang K, Tian Y, Li M, et al. Performance of a multileaf collimator system for a 1.5T MR-linac. *Med Phys*. 2021;48(2):546–555. doi:10.1002/mp.14608.
76. Adler JR, Chang SD, Murphy MJ, et al. The Cyberknife: a frameless robotic system for radiosurgery. *Stereotact Funct Neurosurg*. 1997;69(1–4):124–128. doi:10.1159/000099863.
77. Jaffray DA, Siewerdsen JH, Wong JW, et al. Flat-panel cone-beam computed tomography for image-guided radiation therapy. *Int J Radiat Oncol Biol Phys*. 2002;53(5):1337–1349. doi:10.1016/s0360-3016(02)02884-5.
78. Shirato H, Shimizu S, Shimizu T, et al. Real-time tumour-tracking radiotherapy. *Lancet*. 1999;353(9161):1331–1332. doi:10.1016/S0140-6736(99)00700-X.
79. Mackie TR, Balog J, Ruchala K, et al. Tomotherapy. *Sem Radiat Oncol*. 1999;9(1):108–117. doi:10.1016/s1053-4296(99)80058-7.
80. Liu Z, Fan J, Li M, et al. A deep learning method for prediction of three-dimensional dose distribution of helical tomotherapy. *Med Phys*. 2019;46(5):1972–1983. doi:10.1002/mp.13490.
81. Xu S, Wu Z, Yang C, et al. Radiation-induced CT number changes in GTV and parotid glands during the course of radiation therapy for nasopharyngeal cancer. *Br J Radiol*. 2016;89(1062):20140819. doi:10.1259/bjr.20140819.
82. Kluter S. Technical design and concept of a 0.35 T MR-linac. *Clin Transl Radiat Oncol*. 2019;18:98–101. doi:10.1016/j.ctro.2019.04.007.
83. LeCun Y, Bengio Y, Hinton G. Deep learning. *Nature*. 2015;521(7553):436–444. doi:10.1038/nature14539.
84. Zhao W, Shen L, Han B, et al. Markerless pancreatic tumor target localization enabled by deep learning. *Int J Radiat Oncol Biol Phys*. 2019;105(2):432–439. doi:10.1016/j.ijrobp.2019.05.071.
85. Zhao W, Han B, Yang Y, et al. Visualizing the invisible in prostate radiation therapy: markerless prostate target localization via a deep learning model and monoscopic kV projection X-ray image. *Int J Radiat Oncol Biol Phys*. 2018;102(3):S128–S129 suppl 1. doi:10.1016/j.ijrobp.2018.06.319.
86. Isaksson M, Jalden J, Murphy MJ. On using an adaptive neural network to predict lung tumor motion during respiration for radiotherapy applications. *Med Phys*. 2005;32(12):3801–3809. doi:10.1118/1.2134958.
87. Kakar M, Nystrom H, Aarup LR, et al. Respiratory motion prediction by using the adaptive neuro fuzzy inference system (ANFIS). *Phys Med Biol*. 2005;50(19):4721–4728. doi:10.1088/0031-9155/50/19/020.
88. Murphy MJ, Pokhrel D. Optimization of an adaptive neural network to predict breathing. *Med Phys*. 2009;36(1):40–47. doi:10.1118/1.3026608.
89. Valdes G, Scheuermann R, Hung CY, et al. A mathematical framework for virtual IMRT QA using machine learning. *Med Phys*. 2016;43(7):4323. doi:10.1118/1.4953835.
90. Carlson JN, Park JM, Park SY, et al. A machine learning approach to the accurate prediction of multi-leaf collimator positional errors. *Phys Med Biol*. 2016;61(6):2514–2531. doi:10.1088/0031-9155/61/6/2514.
91. Li Q, Chan MF. Predictive time-series modeling using artificial neural networks for linac beam symmetry: an empirical study. *Ann N Y Acad Sci*. 2017;1387(1):84–94. doi:10.1111/nyas.13215.
92. Li J, Wang L, Zhang X, et al. Machine learning for patient-specific quality assurance of VMAT: prediction and classification accuracy. *Int J Radiat Oncol Biol Phys*. 2019;105(4):893–902. doi:10.1016/j.ijrobp.2019.07.049.
93. Valdes G, Chan MF, Lim SB, et al. IMRT QA using machine learning: a multi-institutional validation. *J Appl Clin Med Phys*. 2017;18(5):279–284. doi:10.1002/acm2.12161.

94. Chan MF, Witztum A, Valdes G. Integration of AI and machine learning in radiotherapy QA. *Front Artif Intell.* 2020;3:577620. doi:10.3389/frai.2020.577620.
95. Zhao W, Patil I, Han B, et al. Beam data modeling of linear accelerators (linacs) through machine learning and its potential applications in fast and robust linac commissioning and quality assurance. *Radiother Oncol.* 2020;153:122–129. doi:10.1016/j.radonc.2020.09.057.
96. Fan J, Xing L, Ma M, et al. Verification of the machine delivery parameters of a treatment plan via deep learning. *Phys Med Biol.* 2020;65(19):195007. doi:10.1088/1361-6560/aba165.
97. Fan J, Xing L, Yang Y. Independent verification of brachytherapy treatment plan by using deep learning inference modeling. *Phys Med Biol.* 2021;66(12). doi:10.1088/1361-6560/ac067f.
98. Keall PJ, Sawant A, Berbeco RI, et al. AAPM Task Group 264: The safe clinical implementation of MLC tracking in radiotherapy. *Med Phys.* 2021;48(5):e44–e64. doi:10.1002/mp.14625.
99. Ibragimov B, Toesca DA, Yuan Y, et al. Deep 3D dose analysis for prediction of outcomes after liver stereotactic body radiation therapy. In: Frangi A, Schnabel J, Davatzikos C, Alberola-López C, Fichtinger G, eds. *Medical Image Computing and Computer Assisted Intervention – MICCAI 2018. Lecture Notes in Computer Science.* Vol 11071. Springer;2018:684–692. doi:10.1007/978-3-030-00934-2\_76.
100. Ibragimov B, Toesca DAS, Chang DT, et al. Deep learning for identification of critical regions associated with toxicities after liver stereotactic body radiation therapy. *Med Phys.* 2020;47(8):3721–3731. doi:10.1002/mp.14235.
101. Bibault JE, Chang DT, Xing L. Development and validation of a model to predict survival in colorectal cancer using a gradient-boosted machine. *Gut.* 2021;70(5):884–889. doi:10.1136/gutjnl-2020-321799.
102. Liu J, Yang L, Zhang JL, et al. Integrate sequence information of dose volume histogram in training LSTM-based deep learning model for lymphopenia diagnosis. *Int J Radiat Oncol Biol Phys.* 2021;111(3):e112–e113. doi:10.1016/j.ijrobp.2021.07.520.
103. Appelt AL, Elhaminia B, Gooya A, et al. Deep learning for radiotherapy outcome prediction using dose data - a review. *Clin Oncol (R Coll Radiol).* 2022;34(2):e87–e96. doi:10.1016/j.clon.2021.12.002.
104. Cruz Rivera S, Liu X, Chan AW, et al. Guidelines for clinical trial protocols for interventions involving artificial intelligence: the SPIRIT-AI extension. *Nat Med.* 2020;26(9):1351–1363. doi:10.1038/s41591-020-1037-7.
105. Liu X, Rivera SC, Moher D, et al. Reporting guidelines for clinical trial reports for interventions involving artificial intelligence: the CONSORT-AI Extension. *BMJ.* 2020;370:m3164. doi:10.1136/bmj.m3164.
106. Luo W, Phung D, Tran T, et al. Guidelines for developing and reporting machine learning predictive models in biomedical research: a multidisciplinary view. *J Med Internet Res.* 2016;18(12):e323. doi:10.2196/jmir.5870.
107. Rodríguez-Barroso N, Stipcich G, Jiménez-López D, et al. Federated learning and differential privacy: software tools analysis, the Sherpa.ai FL framework and methodological guidelines for preserving data privacy. *Info Fusion.* 2020;64:270–292. doi:10.1016/j.inffus.2020.07.009.
108. Shneiderman B. Bridging the gap between ethics and practice. *ACM Trans Interact Intell Syst.* 2020;10(4):1–31. doi:10.1145/3419764.
109. Hagendorff T. The ethics of AI ethics: an evaluation of guidelines. *Minds Machs.* 2020;30(1):99–120. doi:10.1007/s11023-020-09517-8.
110. Jobin A, Ienca M, Vayena E. The global landscape of AI ethics guidelines. *Nat Mach Intell.* 2019;1(9):389–399. doi:10.1038/s42256-019-0088-2.